Ab Initio Exploration of Rearrangement Reactions: Intramolecular Hydrogen Scrambling Processes in Acetone

Clotilde S. Cucinotta,[†,‡] Alice Ruini,[‡,§] Alessandra Catellani,[#,§] and András Stirling*[,⊥]

National Center on nanoStructures and bioSystems at Surfaces (S[2]) of INFM-CNR, Modena, Italy; Dipartimento di Fisica, Universita di Modena e Reggio Emilia, Modena, Italy; CNR-IMEM, Parma, Italy; and Chemical Research Center, Budapest, Hungary

Received: July 6, 2006; In Final Form: October 24, 2006

The recently developed metadynamics method is applied to the intramolecular hydrogen migration reactions of acetone in the gas phase. Comparison of different sets of collective coordinates allows efficient description of the underlying free energy surface. The simulations yielded numerous reactions: the enol−oxo tautomerism, the decomposition of acetone to various products, and rearrangement reactions. On the basis of the calculated activation barriers it is concluded that the enol−oxo tautomerism is the most frequent intramolecular proton-exchange process the acetone undergoes in the gas phase.

I. Introduction

In this study we address the problem of simulating parallel chemical reactions by finite temperature methods. The principal problem we face when modeling chemical reactions where there is a non-negligible entropy contribution is the problem of the efficient sampling of the reactive path in phase space, because the reactive event is rare on the simulation time scale. Several methods have been proposed to overcome this problem.[1−8] The reaction free energy is usually sampled along a predefined path. Identifying the proper reaction coordinate is, however, a delicate issue: it often involves several internal coordinates in a complex time-dependent manner. An incomplete choice leads inevitably to an overestimated barrier.

Obviously the simulation becomes much less biased if we are allowed to select not only one but several reaction coordinates and the free energy surface (FES) is sampled in the space spanned by these variables. In fact, the recently developed metadynamics method offers such a framework: the system finds the lowest energy reaction path through the combined action of several collective variables (CVs) and at the same time the simulation yields the free energy with regard to these variables. Detailed description of the metadynamics can be found in refs 9−12 as well as in the next section of this work.

In a complete metadynamics simulation not only the lowest path but also the higher energy, less likely, reaction routes are also found. The reaction mechanisms identified from the simulation can be considered as a path in the space of the selected CVs. Thus, selection of other sets of coordinates or increase of the dimension of the "reaction space" by involving new coordinates leads to the observation of further reactions during the simulation. With this strategy one can very efficiently explore the lowest, competitive paths and discover new routes that may become competitive after proper chemical modifications are introduced into the reactant molecules. The true reaction coordinate associated with an observed process can be obtained if all of the relevant slow motions are included in the CV set.

In a recent study we have thoroughly investigated the water-catalyzed tautomer interconversion of acetone.[13] Besides the intermolecular mechanism we have also studied the gas-phase intramolecular tautomerism. In general, several different intramolecular proton-exchange reactions can be devised, besides the tautomeric reaction. From the industrial point of view other hydrogen-exchange reactions leading to the decomposition of acetone, such as the thermal cracking of acetone producing ketene, are also important.[14]

In this study we model these hydrogen-exchange processes by applying the metadynamics method. We have explored the FES along several different degrees of freedom and observed the tautomeric equilibrium, two different dehydration mechanisms, and the double-bond shift by proton exchange between the methyl and methylene groups of the enol form as well as the high-energy decomposition of acetone to ketene and methane. In what follows we show the remarkable ability of the metadynamics to find these characteristically different routes along with the corresponding activation barriers.

II. Theoretical Method

A. Metadynamics: Technical Details. The metadynamics[9] is an artificial dynamics in the space defined by few CVs, $s(\mathbf{R})$, where $\mathbf{R}$ indicates the ionic degrees of freedom of the system. The fundamental requirement for the CVs is that they have to distinguish between reactants and products. These CVs sample a multidimensional free energy (FE) landscape by searching for the transition to new (and often unexpected) stable and metastable basins. The metadynamics speeds up the sampling of the multidimensional configurational space by introducing a history-dependent potential

$$V_G(s(\mathbf{R}),t) = w \int_0^t \mathrm{d}t' \exp\left(-\frac{|s(\mathbf{R}) - s(\mathbf{R}_G(t'))|^2}{2|\delta s|^2}\right), \quad (1)$$

where w and δs are height and width of the multidimensional Gaussian, respectively, and $\mathbf{R}_G(t')$ is the trajectory of the system under the action of $V(\mathbf{R}) + V_G$, where $V(\mathbf{R})$ is the potential of

* Author to whom correspondence should be addressed.
† Present address: ETHZ, Lugano, Switzerland.
‡ National Center on nanoStructures and bioSystems at Surfaces (S2) of INFM-CNR.
§ Università di Modena e Reggio Emilia.
# CNR-IMEM.
⊥ Chemical Research Center.

10.1021/jp064263c CCC: $33.50
Published on Web 12/21/2006

the system. If τ_G is the temporal distance between two successive Gaussians, $V_G(s(\mathbf{R}),t)$ can be seen for $\tau_G \rightarrow 0$ as the limit of a sum of Gaussian functions, centered along the trajectory in the CV space, visited during the evolution of the system. If the Gaussians are added sufficiently slowly, the potential thus fills the FE landscape and biases the system toward the lowest FE barrier. The function

$$F(s(\mathbf{R}),t) = -V_G(s(\mathbf{R}),t) \tag{2}$$

evaluates the FE of the system[15] in the region of space explored up to time t: the accuracy of the procedure is proportional to the inverse square of the diffusion time required to visit the basin of interest.[11]

The coupling between *macroscopic* (relative to s) and *microscopic* (relative to R) dynamics is realized in a continuous way within the Iannuzzi, Laio, and Parrinello extended Lagrangian scheme:[10] within this scheme an auxiliary variable S_i is introduced for each $s_i(\mathbf{R})$ CV in the configurational space. The Lagrangian of the system is

$$L = L_{\mathrm{CP}} + \sum_i \left(\frac{1}{2}\right) M_i \dot{S}_i^2 - \sum_i \left(\frac{1}{2}\right) k_i (s_i(\mathbf{R}) - S_i)^2 - V_G(S,t) \tag{3}$$

where L_{CP} is the Car−Parrinello Lagrangian; the first additional term, $\sum_i (^1/_2) M_i \dot{S}_i^2$, represents the fictitious kinetic energy of the S_i values, and M_i is the corresponding fictitious mass parameter; the second additional term, $\sum_i (^1/_2) k_i (s_i(\mathbf{R}) - S_i)^2$, represents a restraining potential that forces the ionic degrees of freedom to follow the motion of the CVs; it can also be seen as a sort of *cage* contribution that allows the relative motion of the S_i to be tuned with respect to the $s_i(\mathbf{R})$; the k_i values are the coupling constants. With sufficiently large M_i and k_i values the extra dynamical variables move slowly on the free energy surface. The last additional term, $V_G(S_i,t)$, is the time-dependent potential, which ensures that the system visits regions of the FES which have not yet been visited, by adding repulsive potential terms in the form of localized Gaussians.

The choice of parameters M, k, w, and s, as well as the time step and temperature, is critical as it allows the three different diffusion timescales, the ones relative to electrons, to ions, and to the CVs, to be combined. As practical rules to tune k_i and M_i it can be said that (1) the larger is M_i, the more *adiabatically decoupled* are the ionic and collective degrees of freedom, but the slower is the evolution of the CV, and (2) the larger is k_i, the closer $s_i(\mathbf{R})$ is to S_i, but the smaller is also the time step that can be used.

In our calculations, each Gaussian hill is added when the CV has diffused at a $(^3/_2)w$ distance from the preceding one. k_i and M_i are chosen so that the instantaneous value $s_i(\mathbf{R})$ remains always close to S_i and the characteristic frequencies of the CVs $\omega_{CV_i} = \sqrt{k_i/M_i}$ are of the same order of the underlying mean ionic modes both in the gas phase and in water. For what concerns the choice of the hill height w and width δs, we first performed preliminary runs by using large values to obtain information about the reactions. Subsequently, we refined our calculations by using smaller hill sizes: the optimal hill height for the evaluation of energy barriers in the described reactions was found to be 2.3 kcal/mol and the width is 0.02 ucv (units of CV). This value is considered as an approximate estimate of the error bar for energy values.[11] The metadynamics method has been already applied successfully for numerous chemical problems, see, for example, refs 13, and 16−18.

B. Choice of the Collective Variables. In a metadynamics simulation we select several CVs and the free energy is explored in the space spanned by these coordinates. It follows that the choice of CVs determines the possible directions of the reaction paths that can be observed during the simulation, and in the same time excludes those which require different degrees of freedom to be activated. In practice the CVs are represented by continuous functions. We found that in the present case the most appropriate type of CVs to describe the various proton-exchange processes is the coordination number (CN): it is defined as a continuous function of R_{ij} values (the distance between atoms i and j) as

$$\mathrm{CN}_i = \sum_{j=1}^{n} \left(\frac{1 - \left(\frac{R_{ij}}{d_0}\right)^p}{1 - \left(\frac{R_{ij}}{d_0}\right)^q} \right)$$

where i corresponds to the reference atom, j runs over the atoms coordinated to the reference atom, and d_0 represents a reference distance (the ideal d_0 value is close to the distance in the transition state). p and q determine the decay of the CN curve. We note that this decay can affect significantly the evolution of the estimated free energy surface in the simulations.

C. Computational Details. We performed molecular dynamics (MD) simulations from first principles[19] within the density-functional theory scheme, using the BLYP exchange correlation functionals;[20] we used ultrasoft pseudopotentials with a plane wave basis set expanded to a 25 Ry energy cutoff at the Γ point. The reliability of the BLYP functional for the present study has been checked by performing two separate sets of static BLYP and B3LYP[21] calculations a posteriori using the Gaussian 03 program package[22] employing the 6-311++g** basis set. The two methods give the same ordering for the barrier heights and a 7.0% mean relative deviation with respect to the BLYP activation energy values, which confirms nicely our methodology. The input configurations are obtained using the PCFF empirical force field;[23] ab initio structural relaxations are then performed until the forces vanish within 0.001 eV/Å. The isolated molecule is simulated in a supercell geometry in an otherwise empty cell of 18 × 18 × 18 Å^3, which prevents significant interactions between replicas. Free energy barriers of the various reaction routes are then calculated within the metadynamics approach.

III. Results

The various proton scramblings can be classified as hydrogen exchange between the oxygen and the terminal carbon atoms and exchange between the two terminal C atoms. To observe and describe the possible routes we have employed three sets of CVs.

1. The first set is composed of two CVs: the CN of a single terminal C atom with respect to its hydrogens and the CN of oxygen with respect to the same hydrogen atoms. This set is obviously asymmetric: it excludes one of the methyl groups from the reactions and inhibits a possible proton exchange between the C atoms.

2. The second set also features two CVs: the two individual CNs of the methyl C atoms with respect to all six hydrogen atoms. This choice steers the hydrogen scrambling between the terminal carbon atoms. Such a choice allows one to decide whether the O protonation is a fast process as we implicitly assume that it does not need to be treated explicitly.

TABLE 1: Energy Barriers and Reaction Enthalpies

reaction	barrier (kcal/mol)	reaction enthalpy (kcal/mol)
oxo → enol	57.6	11.8
enol → H_2O + allene	69.0	21.7
enol → H_2O + propyne	78.4	24.4
enol → enol	69.0	0.0
oxol → CH_4 + ketene	80.7	16.9

3. The third set consists of three CVs: the three CNs of the terminal C atoms and the O atom with respect to all six hydrogen atoms. This set involves all of the previous reaction coordinates and lets them compete: during their simultaneous operation the lowest energy path will be explored first. Employing this set we reduce the bias along a predefined configurational subspace. Indeed, this set (i) reflects the molecular symmetry, (ii) boosts the O protonation as well, and (iii) allows quantitative comparison of the barriers obtained with the previous choices.

The calculated activation barriers, together with the reaction enthalpies, are listed in Table 1.

In a typical simulation we start the exploration of the FES at a local minimum: in the basin corresponding to the oxo form. In general, the metadynamics algorithm fills the initial basin with the time-dependent potential. When the basin is sufficiently filled, the system flows into the next basin separated by the reaction barrier. Then this basin starts to fill. Depending on the relative heights of the barriers surrounding this basin, the system will either recross and arrive at the initial basin or explore further basins. Then the process continues, and eventually reactions with very high barriers can be observed. This is a general feature of the metadynamics: within a simulation the reaction channels are explored in the ascending order of the corresponding activation barriers.

Using the first set of CVs, we have first observed the oxo−enol tautomeric rearrangement. After a couple of recrossings, that is, after several enol−oxo tautomer interconversions, we have seen a second, higher energy process initiated from the enol configuration: an additional proton jumped from the methylene to the hydroxyl group, yielding H_2O and propyne. Then the products separated quickly (activation barrier = 78.4 kcal/mol). To verify the methodology, we have performed a metadynamics simulation starting from the enol structure. This simulation provided the same barriers and relative stabilities as the previous one (within the numerical accuracies).

With the second set of CVs, we could observe only one reaction: after one hydrogen atom had transferred from one of the methyl groups to the other, a methane molecule formed, leaving ketene as byproduct. The reaction barrier is very high, 80.7 kcal/mol.

The third set offered a couple of interesting proton-scrambling reactions: tautomerism, double-bond shift, and decomposition. The evolution of the CVs and the FES obtained in the simulation are plotted in Figures 1 and 2, respectively. The elementary steps that could be observed are displayed in Figure 3. The first processes we have observed are the oxo−enol and enol−oxo tautomeric processes. In the next stage an enol−enol transformation via two subsequent proton jumps could be observed: the OH group passes the proton to the methylene group, while the methyl group saturates the oxygen atom, and we obtained the same enol molecule in another conformer state. Then we have seen a proton exchange between the terminal C atoms of the enol form: the interconversion of the methylene and methyl groups is accompanied by the transfer of the double bond from one side to the other. The activation barrier of this process is 69 kcal/mol. Similarly to the previous transformation, this

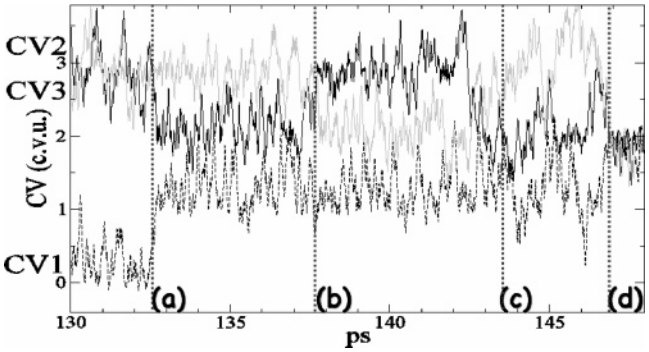

Figure 1. Time evolution of the third set of collective variables. Dashed lines separate different basins visited during the simulation, labeled as in Figures 2 and 3.

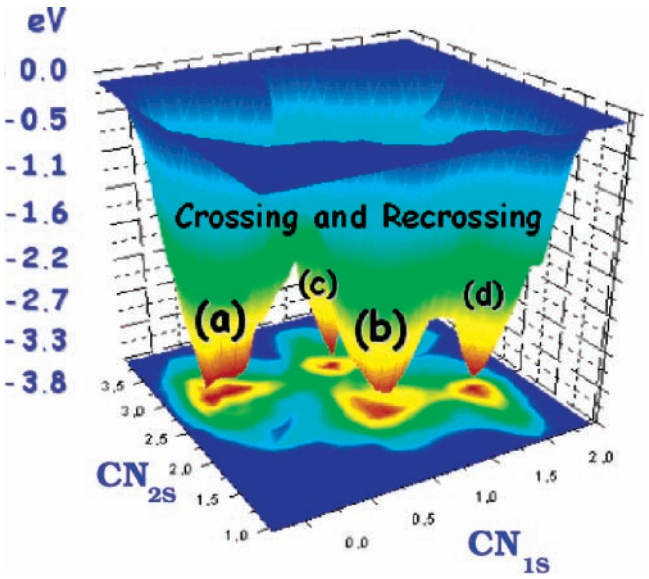

Figure 2. Free energy surfaces (FES) of the system. FES employing the third set of collective variables is plotted as a function of the two CNs of the terminal carbon atoms. Note that for the two-dimensional representation of the free energy we integrated over the third coordinate. Labels refer to different basins visited during the simulation, as in Figures 1 and 3.

reaction is also degenerate: we obtain the enol configuration, although the hydrogens are rearranged. Finally, the effect of the history-dependent potential provokes the decomposition of the molecule, starting from the enol form: in this time the H_2O elimination is accompanied by the formation of allene (propadyene). The activation energy is the same as the previous rearrangement: 69 kcal/mol within the error bar of the simulation. Note that we did not observe these lower energy routes with the previous sets: in those simulations the system was not biased in this direction. In other words, the selected CVs, and not the barrier height of the various possible routes, determine the outcome of a metadynamics simulation.

Comparison of the different runs shows that the most likely intramolecular proton-exchange process in the gas phase is the enol−oxo tautomerism. The other reactions require much higher activation energies: they can occur only at higher temperature. The simulations provided further information about the tautomeric process. The metadynamics run employing the first set of CVs revealed the concerted nature of the C−H bond breaking and O−H bond formation in the enolization process in the gas phase (see also ref 13). The simulation using the second set of CVs (only C−H coordination numbers) provided additional support for this mechanism: the decomposition to ketene and

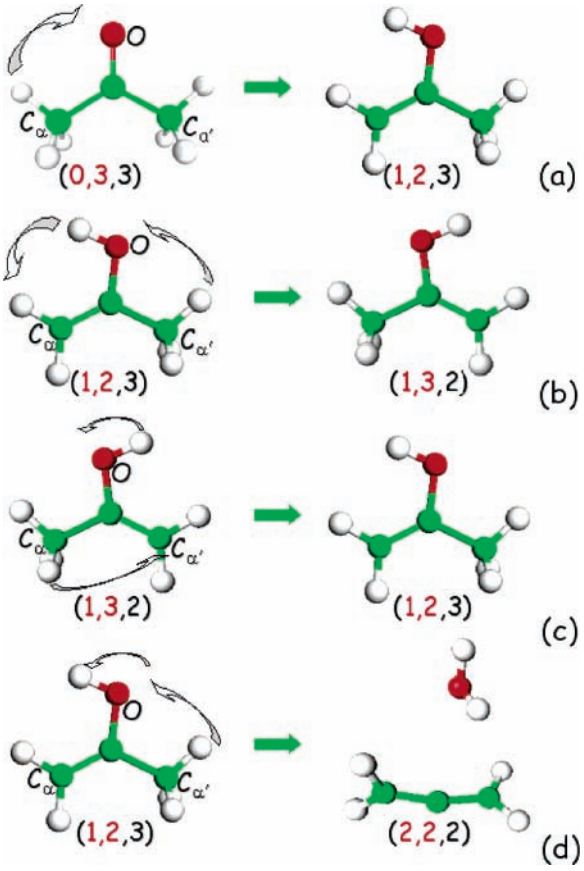

Figure 3. Elementary steps from the trajectory obtained with the third set of CV: (a) deprotonation of the C_a atom of the acetone molecule and in the subsequent enolization of the molecule; (b) enol−enol rearrangement via OH and methyl group deprotonation; (c) enol−enol rearrangement via proton exchange between the terminal C atoms; (d) additional proton transfer to the OH group yields water and allene (propadyene). The numbers in parentheses indicate the values assumed by the CVs along the trajectory, for each snapshot.

CH_4 exhibits a much higher activation energy than the enolization; still, the latter process cannot be observed in this simulation. Whereas both the decomposition and the enolization involve C−H bond breaking, the enolization requires also O−H protonation, which represents a significant barrier in the free energy space. As the time-dependent potential of the second metadynamics run did not boost the reaction in that direction, enolization could not be observed.

In the final scheme (Figure 4) we summarize the reaction paths obtained from the metadynamics along with the corresponding energy barriers (in kilocalories per mole). Clearly, as far as the gas-phase proton-transfer reactions are concerned, no other reaction can compete with the tautomerism, either from the kinetic or from the thermodynamic point of view. On the other hand, among the reactions displayed in Figure 4, the ketene formation is the most important from a synthetic point of view, as it is a very important starting material for the synthesis of various organic compounds. In industrial ketene production the acetone thermally decomposes to ketene + CH_4. The experimental reaction kinetics of this pyrolytic process includes numerous intermolecular steps;[14] therefore, direct comparison cannot be made with our results, but it is clear that thermodynamically the formation of ketene is favored (Table 1) besides the enol−oxo equilibrium, and this tendency is enhanced by the high experimental temperature (ca. 1000 K). Notwithstanding the other reactions are also important as they are the reverse of the basic addition reaction processes:

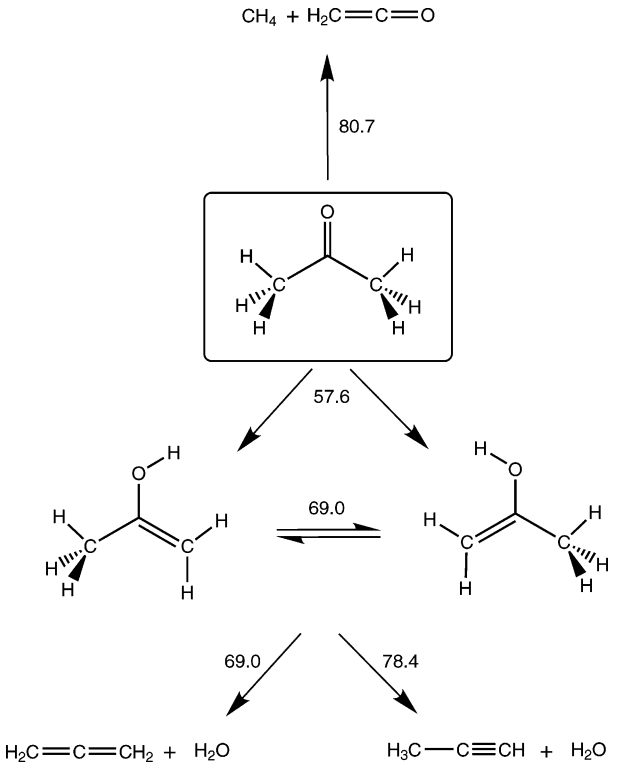

Figure 4. Various paths of proton exchange in gas-phase acetone. Activation energies are in kilocalories per mole.

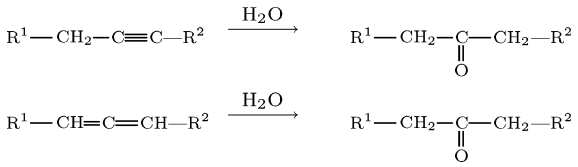

The above reactions represent in general the water addition on terminal cumulated double bonds and on triple bonds. In the simplest case, when R^1 and R^2 are hydrogens, our reaction paths are recovered. These *nonradical* reactions are of high industrial importance. Our simulations provide the corresponding reaction paths for these processes, albeit in a backward manner. This points to an essential feature of the metadynamics method: the mechanism that governs the system toward a thermodynamical sink can be recovered by simulating the back route with metadynamics. In principle, a simulation started from the product side may not necessarily yield the expected reactants, but may recover a lower energy route toward more stable initial compounds. In this context our study points out two particularly intriguing aspects of the simulations: (i) we could recover the most common synthetic paths of acetone from hydrocarbons and (ii) the selected set of CVs essentially affects the outcome of the simulation: all of the observed elementary steps having barriers higher than the thermal energy available in the system will be a linear combination of the selected CVs. In turn, no other elementary steps with higher barriers can be seen in the simulation. This is the why we have obtained different routes from the simulations.

IV. Conclusions

In summary, we have carried out a series of ab initio simulations in the metadynamics frame to describe the various thermal intramolecular rearrangements of acetone. The main feature of these reactions is that they scramble the hydrogen atoms among the methyl and oxo groups. We have observed

the enol−oxo tautomerism equilibrium, proton exchange between the methyl and methylene groups of the enol form, and three different decomposition processes: formation of ketene + CH_4 and formation of allene or propyne by water elimination. The energetics of the elementary steps suggests that in the gas phase the most frequent intramolecular rearrangement of acetone is the enol−oxo tautomerism.

Acknowledgment. We are grateful to Stefano Corni and Elisa Molinari for fruitful discussion. Computer time was partly provided by CINECA through INFM Parallel Computing Projects and CSCS (Manno, CH). The support by the RTN EU Contract "EXCITING" No. HPRN-CT-2002-00317 and by FIRB "NOMADE" is also acknowledged.

References and Notes

(1) Ren, W. E. W.; Vanden-Eijnden, E. *Phys. Rev. B* **2002**, *66*, 052301.
(2) Merlitz, H.; Wenzel, W. *Chem. Phys. Lett.* **2002**, *362*, 271−277.
(3) Huber, T.; Torda, A.; van Gusteren, W. *J. Comput.-Aided Mol. Design* **1994**, *6*, 695−708.
(4) Carter, E. A.; Ciccotti, G.; Hynes, J. T.; Kapral, R. *Chem. Phys. Lett.* **1989**, *156*, 472−477.
(5) Sprik, M.; Ciccotti, G. *J. Chem. Phys.* **1998**, *109*, 7737−7744.
(6) Torrie, G. M.; Valleau, J. P. *J. Comput. Chem.* **1977**, *23*, 187−199.
(7) Darve, E.; Pohorille, A. *J. Chem. Phys.* **2001**, *115*, 9169−9183.
(8) Dellago, C.; Bolhuis, P. G.; Csajka, F. S.; Chandler, D. *J. Chem. Phys.* **1998**, *108*, 1964−1977.
(9) Laio, A.; Parrinello, M. *Proc. Natl. Acad. Sci. U.S.A.* **2002**, *99*, 12562−12566.
(10) Iannuzzi, M.; Laio, A.; Parrinello, M. *Phys. Rev. Lett.* **2003**, *90*, 238302.
(11) Laio, A.; Rodriguez-Fortea, A.; Gervasio, F. L.; Ceccarelli, M.; Parrinello, M. *J. Phys. Chem. B* **2005**, *109*, 6714−6721.
(12) Ensing, B.; Laio, A.; Parrinello, M.; Klein, M. L. *J. Phys. Chem. B* **2005**, *109*, 6676−6687.
(13) Cucinotta, C. S.; Ruini, A.; Catellani, A.; Stirling, A. *ChemPhysChem* **2006**, *7*, 1229−1234.
(14) Sato, K.; Hidaka, Y. *Combust. Flame* **2000**, *122*, 291−311.
(15) Bussi, G.; Laio, A.; Parrinello, M. *Phys. Rev. Lett.* **2006**, *96*, 090601.
(16) Stirling, A.; Iannuzzi, M.; Laio, A.; Parrinello, M. *ChemPhysChem* **2004**, *5*, 1558−1568.
(17) Stirling, A.; Iannuzzi, M.; Parrinello, M.; Molnar, F.; Bernhart, V.; Luinstra, G. A. *Organometallics* **2005**, *24*, 2533−2537.
(18) Ensing, B.; De Vivo, M.; Liu, Z.; Moore, P.; Klein, M. L. *Acc. Chem. Res.* **2006**, *39*, 73−81.
(19) CPMD V3.9.2 (Copyright IBM Corp 1990−2001, Copyright MPI für Festkörperforschung Stuttgart 1997−2001), http://www.cpmd.org.
(20) Becke, A. D. *Phys. Rev. A* **1988**, *38*, 3098−3100. Lee, C.; Yang, W.; Parr, R. G. *Phys. Rev. B* **1988**, *37*, 785−789.
(21) Becke, A. D. *J. Chem. Phys.* **1993**, *98*, 5648−5652. Lee, C. T.; Yang, W. T.; Parr, R. G. *Phys. Rev. B* **1988**, *37*, 785−789.
(22) Frisch, M. J., et al. *Gaussian 03*, revision C.01; Gaussian, Inc.: Wallingford, CT, 2004.
(23) Hwang, M. J.; Stockfisch, T. P.; Hagler, A. T. *J. Am. Chem. Soc.* **1994**, *116*, 2515−2525.